A stochastic simulation-based approach for sizing DRES penetration level and BESS capacity in distribution grids

Aihui Fu [a,*], Aleksandra Lekić [a], Kyriaki-Nefeli D. Malamaki [b], Georgios C. Kryonidis [b], Juan M. Mauricio [c], Charis S. Demoulias [b], Peter Palensky [a], Miloš Cvetković [a]

[a] Department of Electrical Sustainable Energy, Delft University of Technology, Mekelweg 4, Delft, 2628CD, The Netherlands
[b] Department of Electrical & Computer Engineering, Aristotle University of Thessaloniki, Aristotle University of Thessaloniki, Thessaloniki, 54124, Greece
[c] Department of Electrical Engineering, University of Seville, Camino de los Descubrimientos, Seville, 41092, Spain

A B S T R A C T

The extensive integration of distributed renewable energy resources (DRES) can lead to several issues in power grids, particularly in distribution grids, due to their inherent intermittency. This paper presents a stochastic simulation-based approach to estimate the maximum permissible penetration level of DRES and to determine the optimal capacity of centralized battery energy storage systems (BESS) in distribution networks while adhering to technical constraints. The stochastic method creates a wide range of scenarios under various conditions. For each scenario, our proposed approach calculates the maximum allowable penetration level of DRES and the required BESS capacity with different DRES control logics. The maximum allowable penetration level of DRES and the requirements of the BESS capacity are determined by an analysis of various simulation results. This paper's unique contribution lies in equipping distribution system operators (DSOs) with the ability to compare results and select the most appropriate voltage control and power smoothing methods. This aids in mitigating challenges associated with overvoltage and intermittency issues arising from DRES-generated power, thereby enhancing the overall resilience and reliability of the power grid. Case studies that include four voltage control algorithms and three power smoothing methods demonstrate the universality and effectiveness of the proposed approach.

1. Introduction

Recently, the adoption of distributed renewable energy sources (DRES) has been increasing to address energy supply shortages during the ongoing energy transition. However, the intermittent, volatile, and uncertain nature of DRES can lead to voltage issues and unstable power supply, which in turn limits the DRES penetration level in distribution networks [1]. Voltage violations in distribution networks with high DRES penetration levels have already attracted researchers' attention, and various conventional and advanced methods have been proposed to address these issues. Conventional voltage control methods include constant Q and $Q(V)$ droop control strategies, as presented in [2]. Ref. [3] proposes a novel control strategy for managing voltage regulators based on a multi-agent system (MAS), while [4] suggests a novel distributed cooperative voltage regulation method for optimal voltage regulation. The voltage profile has been utilized as either an objective or a constraint in the DRES planning problem in [5], with authors determining the maximum DRES penetration level based on a single control method. However, approaches for determining the maximum allowable DRES penetration level considering various conditions and various voltage control logics are still lacking.

The increased intermittency of DRES and the variability of loads compel the transmission system operator (TSO) to manage more energy in the intraday market. Many grid codes impose specific limits on DRES power fluctuations [6], often conservative. As the DRES penetration level increases in the distribution grids, the problem of power fluctuation from the distribution grids to the transmission grids arises. The battery energy storage system (BESS) is commonly employed to mitigate fluctuating power at the upstream distribution grids [7]. A Ramp-rate Limitation algorithm is proposed in [8,9] to smooth the DRES power. A novel controller utilizing a neural network model is suggested for smoothing solar power fluctuations with BESS in [10]. Various smoothing methods and algorithms, as presented in [8–11], and [12], offer methods to obtain more accurate representative days for optimizing BESS size within the optimization horizon. However, there is still a lack of a systematic simulation-based approach to compare different power smoothing methods and size the BESS for power

* Corresponding author.
E-mail address: aihui.fu@outlook.com (A. Fu).

smoothing to achieve high DRES penetration levels.

To address these issues, we propose a stochastic simulation-based approach for assessing and determining the DRES penetration level and Central BESS capacity. We assume the BESS is connected to the substation and the DRES operate under a voltage control scheme. BESS capacity for power smoothing. First, various stochastic scenarios are generated based on existing grid conditions. Then, through the analysis of a variety of simulation results based on each generated scenario, the allowable maximum penetration level of DRES for the distribution network is determined for each voltage control scheme. Finally, an incremental approach is implemented to size the BESS capacity with different power smoothing logic to mitigate the influence of power fluctuations on the external grid.

The main contribution of this paper is that we propose the stochastic simulation-based approach for sizing the DRES penetration level and the central BESS capacity in distribution grids. Firstly, by providing a variety of conditions, voltage control schemes and power smoothing methods, numerous stochastic scenarios can be automatically generated. A comparative analysis of voltage control and BESS power smoothing methods is performed. Second, the risk of technical violation and power smoothing target failure can be analyzed by examining a long period of simulation results. Thirdly, the primary advantage of this approach is that it allows the Distribution Network Operator to assess their preferred voltage regulation and power smoothing methods and decide which one to use based on their network and needs.

The rest of the paper is organized as follows: a detailed explanation of the stochastic simulation-based approach is provided in Section 2. Case studies are presented in Section 3, and concluding remarks are discussed in Section 4.

2. Approach for sizing DRES and BESS

The approach for sizing high DRES penetration level networks is summarized in four steps. Firstly, a large number of scenarios are generated with versatile conditions (DRES installed number, location, and capacity allocation). Secondly, scenario-based results are analyzed using different voltage regulation control schemes to determine a reasonable upper limit for the DRES penetration level. Thirdly, various power smoothing methods are employed by the Central BESS to reduce the influence of power fluctuations caused by high DRES penetration levels. Fourthly, a multitude of simulation results are analyzed to determine the suitable BESS capacity. A single simulation platform cannot achieve the desired goals and verify our proposed sizing methodology. Therefore, we combine Python and PowerFactory [13] to create a simulation platform capable of manipulating data, changing model parameters, and performing simulations.

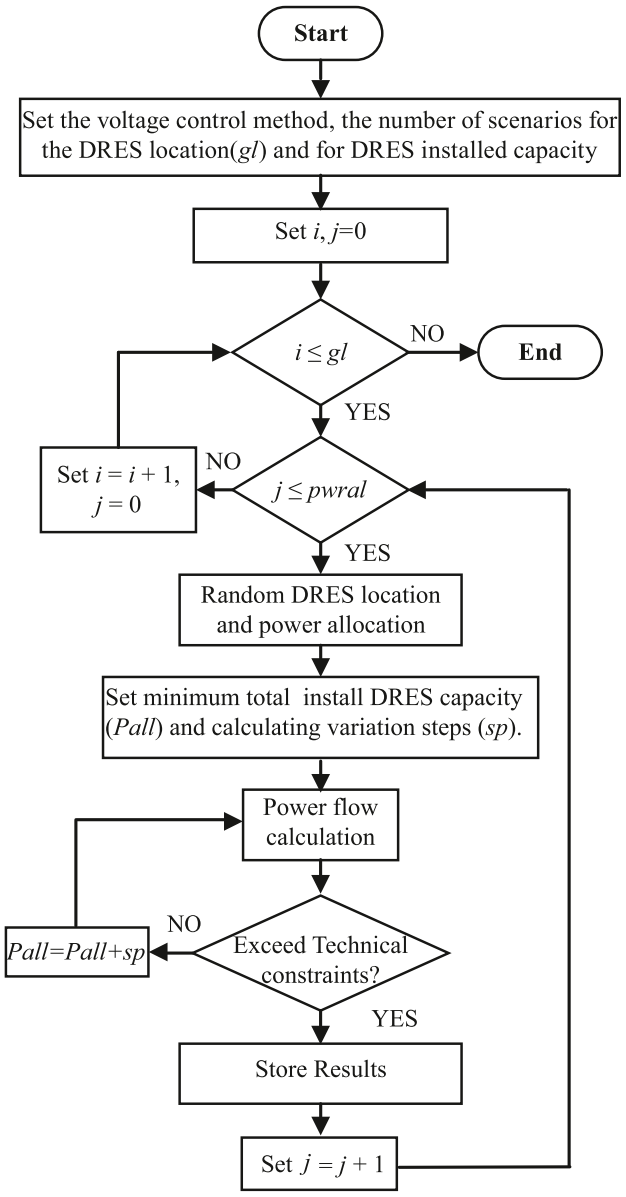

Fig. 1. The flowchart of maximum DRES penetration simulation method.

2.1. Evaluation items and methods

2.1.1. Maximum DRES penetration level determination

The maximum DRES penetration level is defined as the total installed DRES capacity that can be achieved without violating the grid's technical constraints, i.e., the nodes' voltage and the lines' thermal limits. Various combinations of the number of DRES and the number of DRES capacity allocations are assessed, as they can all affect the maximum DRES penetration level. For each combination, an iterative procedure is employed to calculate the maximum penetration level of DRES. In each scenario, the DRES location and power are allocated randomly, and the penetration level of DRES is incrementally increased until the technical constraints are reached. With a given voltage control method and the number of installed DRES, the flow chart of the maximum DRES penetration simulation method is shown in Fig. 1.

In our platform, any voltage control method could serve as input. Still, we only included the most popular decentralized approaches since these are the ones specified in current grid codes and Standards [14, 15], highlighting the practical nature and the applicability of the proposed stochastic simulation-based approach to serve the purpose, which are Constant Q, $PF(P)$ droop control, $Q(P)$ droop control and $Q(V)$ droop control method. In Constant Q mode, the reactive power from DRES is set as a constant value, and in this paper, we set the reactive power as 10% of DRES rated power. In $PF(P)$ droop control mode, the power factor (the ratio of active power to apparent power) of the DRES generator is adjusted based on the generated active power, as shown in Fig. 2. When the DRES active output power is lower than 50% of the rated active power, the power factor is set to one. Conversely, when the DRES output power is higher than 50% of the rated active power, the power factor is set to 0.89. In the $Q(P)$ control droop mode, the reactive power changes based on the generated active power, as illustrated in Fig. 3. In the $Q(V)$ droop mode, the reactive power varies according to the voltage value, with the settings for the $Q(V)$ droop mode shown in Fig. 4. In this mode, the reactive power from DRES follows the voltage values, enabling effective voltage regulation. After the initial setup, a loop is created in which the active power of DRES is incrementally increased by 2 kWp for Low Voltage (LV) grids and 100 kWp for Medium Voltage (MV) grids until voltage or loading violations

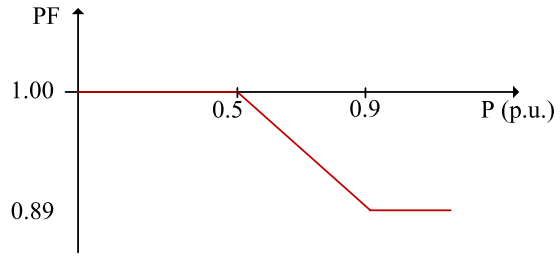

Fig. 2. $PF(P)$ droop control curve [2].

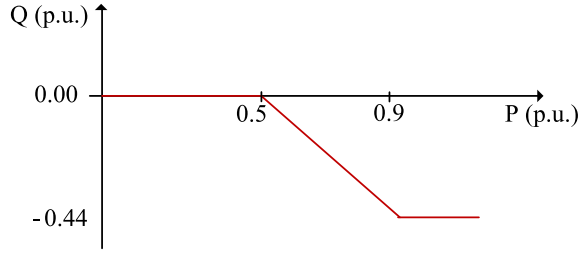

Fig. 3. $Q(P)$ droop control curve [2]. The negative sign indicates operation in the under-excitation mode. That is, DRES absorbs the reactive power.

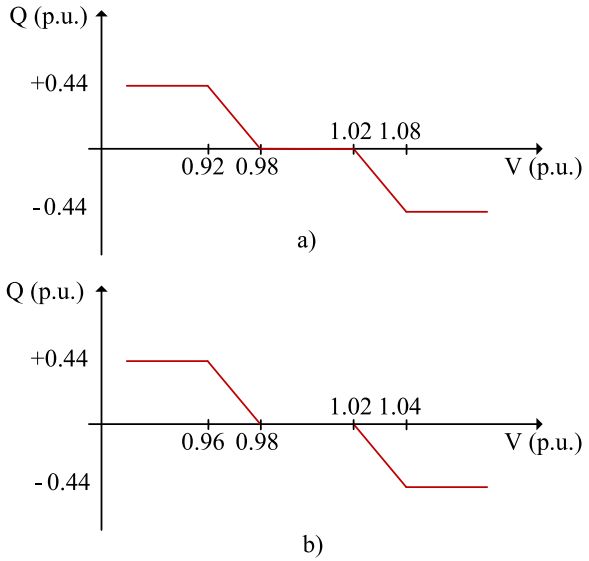

Fig. 4. $Q(V)$ droop control curves [2]: (a) LV grids, and (b) MV grids. The negative sign indicates operation in the under-excitation mode, i.e., DRES absorbs the reactive power.

occur. The last value before the violation(s) is chosen as the maximum DRES power penetration level for the specific scenario. Subsequently, the DSO can compare the results and decide on the most suitable method for their Distribution System.

To determine the maximum penetration level of DRES in power grids, we performed a probability distribution analysis of a large number of results based on different scenarios. However, despite the comprehensive analysis that was conducted to establish the maximum DRES penetration level, there remains a possibility that technical constraints may be exceeded. Therefore, it is essential to investigate the voltage violation risk for a given network, considering the desired installed DRES power, DRES locations, and specified voltage control method.

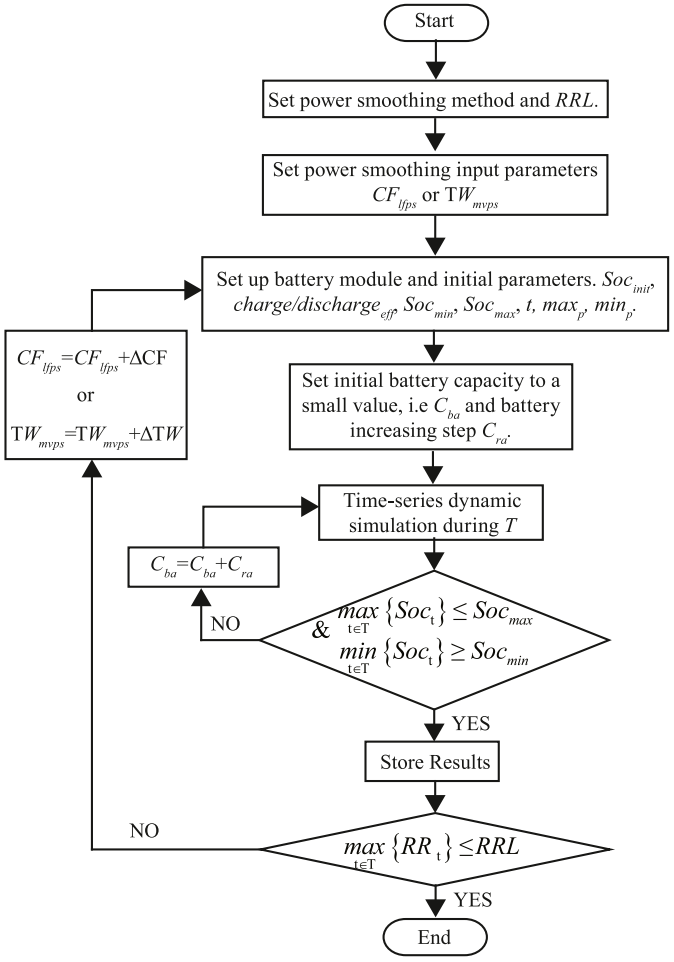

Fig. 5. The flowchart of BESS capacity determination.

To analyze the risk of technical violations, we perform a long-period dynamic simulation (in this paper, we perform a one-year simulation).

2.1.2. Required minimum BESS capacity sizing

To decrease the fluctuation of power at the connection point between the transmission grid and the distribution grids, the BESS is utilized to smooth out the fluctuation power, with the objective of achieving smoother active power profiles injected into the upstream voltage level and enhancing grid stability. Because centralized BESS in the distribution feeder is more effective in managing system-wide issues and easier to control and manage for reliable operation compared with distributed BESS, we use the Central BESS installed upstream of the feeder to perform power smoothing as demonstrated in Ref. [16]. Additionally, the central placement avoids complexities arising from multiple smaller BESS systems. The BESS capacity is determined as the minimum capacity required to meet the ramp-rate limit (RRL) after power smoothing. The platform can determine the BESS capacity based on any power smoothing method. In this paper, we perform simulations based on three popular power smoothing methods: the Moving Average method, the Low-pass Filter method [17], and the Step Ramp-rate Control method [18]. We then compare their results.

The Moving Average is a time series smoothing method that calculates the average of several sequential values of another time series. It is given by:

$$z_t = \frac{1}{k}\sum_{j=0}^{k-1} y_{t-j}, \quad t \in k, k+1, \ldots, n, \tag{1}$$

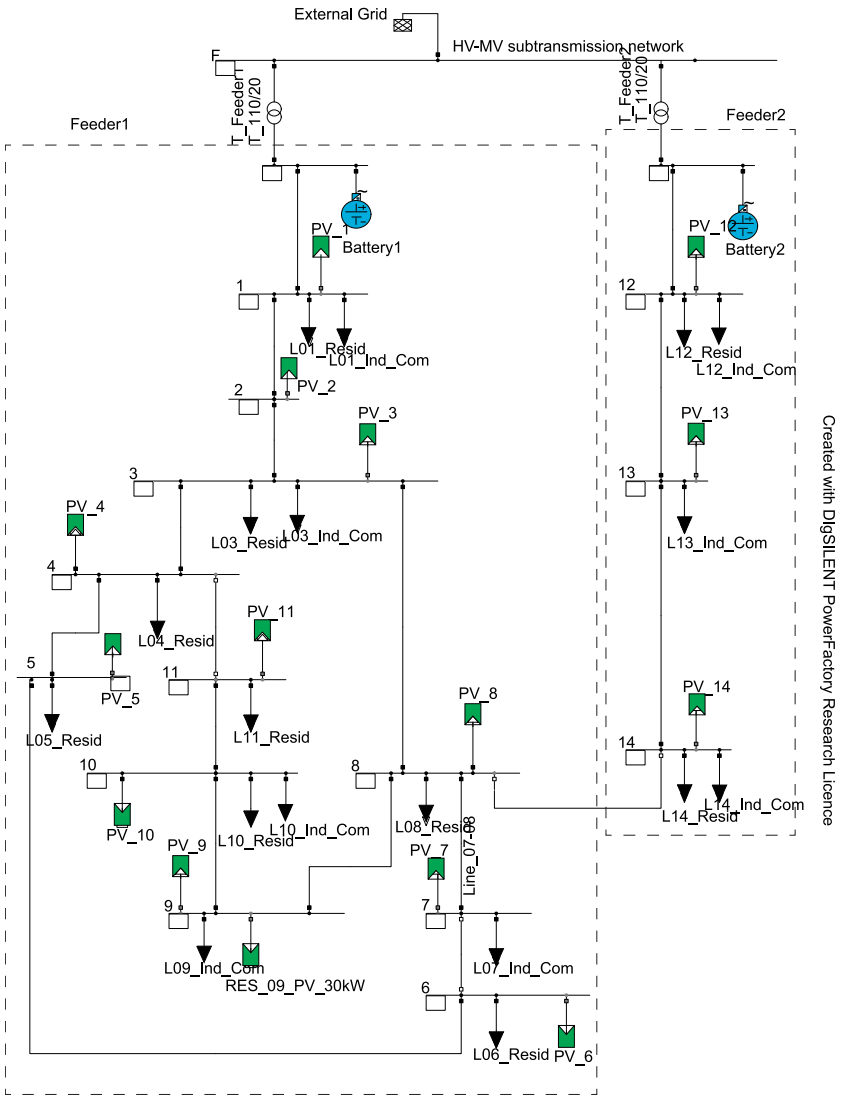

Fig. 6. Cigre MV grid with installed PVs and batteries.

where z_t is the DRES output series power after smoothing, based on the average of the original DRES output series power y_{t-j}. When utilizing the Moving Average method, the window size for the Moving Average method, TW_{mvps}, i.e., the k in Eq. (1), needs to be set.

The Low-pass Filter method is a typical smoothing technique used to remove short-term fluctuations and retain the longer-term trend. It is widely used in DRES power smoothing [17]. The normalized cutoff frequency CF_{lfps} (a number between 0 and 1, representing the ratio of the cutoff frequency to twice the sampling frequency) for the Low-pass Filter method must be set. The transfer function of the Low-pass Filter can be described by:

$$H(s) = \frac{\omega_c}{s + \omega_c} \tag{2}$$

where ω_c is the cutoff angular frequency. In the digital domain, using the normalized cutoff frequency, the transfer function becomes:

$$H(z) = \frac{\pi CF_{lfps}(1 + z^{-1})}{2 + \pi CF_{lfps} + (2 - \pi CF_{lfps})z^{-1}} \tag{3}$$

This expression illustrates how the filter processes the input signal to smooth out short-term variations while preserving the overall trend.

The Step Ramp-rate Control method directly controls the ramp-rate of power within a set limitation [18], which is given by:

$$z_t = \min\left(\max\left(y_t, y_{t-1} - RR \cdot \Delta t\right), y_{t-1} + RRL \cdot \Delta t\right), \tag{4}$$

where RRL is the ramp-rate limitation, and Δt is the sampling time. The y_{t-1} and y_t are the power before smoothing at time $t-1$ and time t, and z_t is the power after smoothing at time t. To use the Step Ramp-rate Control method, the ramp-rate limitation (RRL) must be set.

An iterative procedure will be adopted for different power smoothing methods to calculate the minimum BESS capacity requirement during the simulation time period. The BESS capacity determination flow chart is shown in Fig. 5. The initial set of power smoothing parameters, TW_{mvps} for the Moving Average method and CF_{lfps} for the Low-pass Filter method, should be set as a small value and then iteratively increased with the steps δ_{CF} and δ_{TW} to find the smallest value of TW_{mvps} and CF_{lfps} that meets the ramp-rate limit after power smoothing. The initial BESS capacity, denoted as C_{ba}, should be set at a small value or zero, and the increasing step capacity of BESS is represented as C_{ra}. The settings of the BESS parameters include the name of the BESS, the rated charging and discharging power, the charge and discharge efficiency, the initial state of charge (SoC) and the SoC limitation. The remaining parameters are the simulation time step and simulation period.

The processes of BESS capacity determination are as follows:

- Determine which power smoothing method will be used for the simulation.
- Set the power smoothing method and required value.

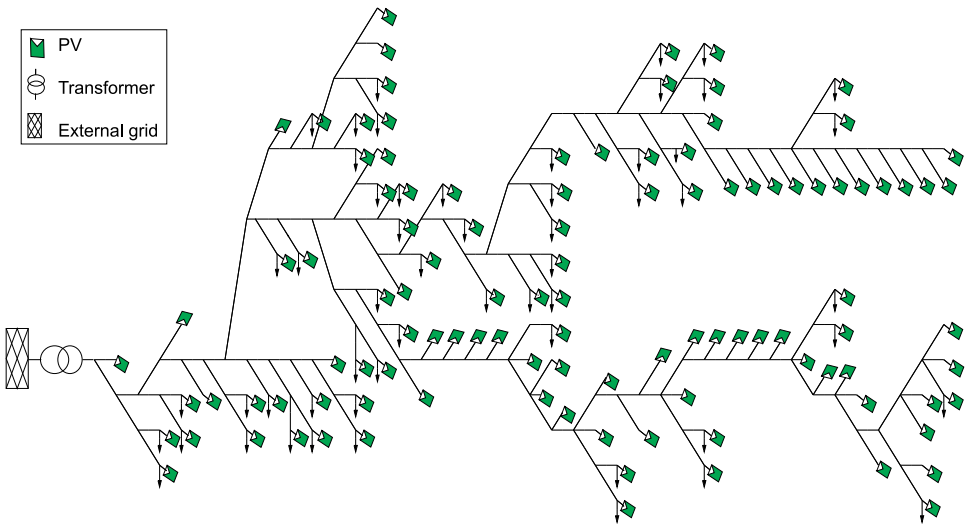

Fig. 7. IEEE LV Test Feeder grid.

- Set up all BESS parameters.
- Perform the dynamic time series simulation during the time period T (simulation period).
- After the simulation, check if the SoC_t (Soc at time t) values in the time period T are all within the limitation. If they are all within the limitation, proceed to the next step; otherwise, increase the BESS capacity and iteratively perform the simulation until the SoC_t values are all within the limit.
- Check if the power after smoothing conforms to the ramp-rate limit standards; if it does, the simulation is complete; otherwise, update the power smoothing parameters and iteratively perform the simulation.

Since the generated power of DRES and load consumption exhibit similar patterns each day, we perform simulations iteratively to determine the BESS capacity requirements for each day. To size the BESS, a large number of minimum BESS required capacities need to be calculated using different load and DRES profiles. As a result, a wide range of scenarios based on varying load and DRES generation profiles in diverse weather conditions and seasons must be simulated. The BESS capacity is then sized as a min–max problem over the entire set of scenarios.

2.2. Simulation platform build up

Our platform is compatible with any network built in PowerFactory. In this paper, the CIGRE network [19] and IEEE European LV Test Feeder [20] are employed as benchmarks for simulation and case studies. Photovoltaic systems (PVs) are installed at each node of the network to represent the DRES for simulation, while BESS are installed upstream of each feeder. The CIGRE MV grid is depicted in Fig. 6, with the BESS named *battery1* and *battery2* in the topology. The IEEE European LV Test Feeder grid is illustrated in Fig. 7. The network model can be imported and applied to the simulation study using Python scripts.

To facilitate the integration of Python with PowerFactory for simulations, DigSILENT PowerFactory includes precompiled Python libraries within its installation folder. For instance, PowerFactory 2024 SP1 supports Python versions 3.8 and 3.9 [13]. Depending on the installed Python version, users can update the dependency in PowerFactory by navigating to TOOLS → Configuration → External applications and specifying the appropriate Python version. To access PowerFactory models, simulate results, and implement the framework functions for studying networks with high DRES penetration levels, a Python class

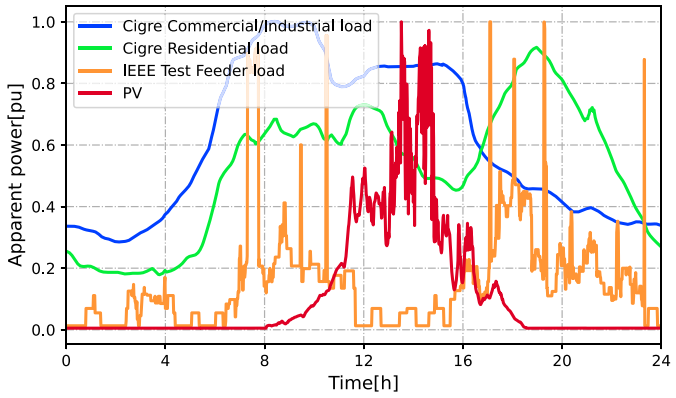

Fig. 8. Daily load and PV profiles of the network [19].

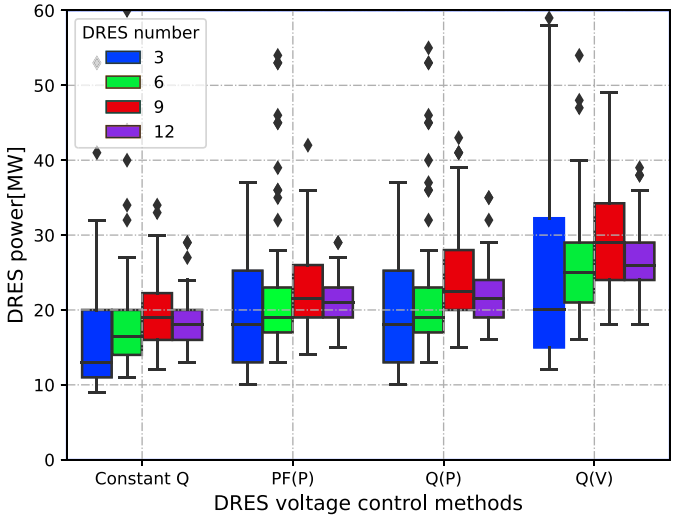

Fig. 9. Maximum DRES penetration level at CIGRE MV network with different voltage control methods and installed DRES number.

named *PowerFactorySim* is developed. This class contains methods to initialize and activate the specific project and study case, functions for power flow and dynamic simulations, creating load and fault events, checking grid technical constraints, and manipulating DRES and BESS parameters. The code is as follows. This integration ensures the simulation platform is flexible, scalable, and capable of addressing various grid scenarios efficiently.

```
import sys
import powerfactory as pf
import os
class PowerFactorySim:
  def __init__(self, folder_name='', project_name='Project',
           study_case='Study Case'):
      # start PowerFactory
      self.app = pf.GetApplication()
      # activate project
      self.app.ActivateProject(os.path.join(folder, project))
      # activate study case
      study_case_folder=self.app.GetProjectFolder('study')
      case=study_case_folder.GetContents(study_case+'.IntCase')
      self.case=case[0]
      self.case.Activate
      ...
   def run_loadflow(self):
      ...
   def get_bus_voltages(self):
     ...
   def get_network_losses(self):
      ...
   def get_DRES_produced_power(self):
     ...
   def get_delivered_upstream_power(self):
    ...
   def check_voltage_violation(self):
    ...
   def check_loading_violation(self):
      ...
   def run_dynamic_sim(self):
      ...
   def set_pv_control(self, PV, control_type):
      ...
   def set_all_loads(self,...):
     ...
   def set_out_of_service(self, elm):
      ...
   def short_circuit(self, ...):
      ...
   def load_event(self, ...):
      ...
   def save_results(self, file='./out.txt'):
      ...
```

3. Case implementations and results analysis

The sizing approach proposed in Section 2 provides methods for assessing the maximum DRES penetration level and BESS capacity. This section evaluates the proposed sizing approach using multiple simulations with different voltage control and power smoothing methods. All simulations are performed on the CIGRE MV benchmark network, shown in Fig. 6, and the IEEE European LV Test Feeder benchmark network, shown in Fig. 7. The load and network information for the CIGRE MV benchmark network and IEEE LV Test Feeder grid follows their official documents [19,20]. The daily PV and load profiles for residential and commercial or industrial loads are shown in Fig. 8. The one-year load and PV profiles for the simulation are obtained from Liander open data [21].

3.1. Case study for maximum DRES penetration level determination

In order to estimate the limit of DRES penetration levels, a significant number of scenarios are generated using our approach. The voltage limit of the network is set to 0.95–1.05 p.u according to EN 50160 standards [22]. To simulate 100 scenarios for each control method (Constant Q, $PF(Q)$, $Q(P)$, and $Q(V)$), the number of different DRES geographic location allocations (gl) is set to 10, and the power allocation scenarios of DRES ($pwral$) is also set to 10.

Using the CIGRE MV grid, we simulate installed DRES numbers of 3, 6, 9, and 12, resulting in a total of 1600 scenarios. For the IEEE European Test Feeder grid, we simulate installed DRES numbers of 10, 20, 30, 40, 50, 60, 70, 80, 90, and 100, yielding a total of 4000 scenarios. This comprehensive set of scenarios allows us to evaluate the maximum DRES penetration level under various conditions, providing valuable insights into the potential of integrating DRES into different network configurations.

3.1.1. Case study with CIGRE MV benchmark grid

In our analysis, a scenario with node voltages exceeding the standard limitation is considered to have a voltage violation problem. Conversely, if all node voltages are within the limit, there is no voltage violation problem. Among the 1600 generated scenarios, only one exhibited a maximum DRES penetration level limited by thermal violation instead of voltage violation. Consequently, our analysis primarily focuses on voltage violation constraints related to the maximum DRES penetration level.

The distribution of maximum accepted DRES capacity in the CIGRE MV grid for all 1600 generated scenarios is depicted in Fig. 9. The figure displays the minimum value, maximum value, lower quartile ($qut1$), mean value (μ), and upper quartile ($qut3$) for specific voltage control methods and DRES numbers. The figure shows that as the number of DRES connections increases, the interquartile range narrows, leading to a tighter clustering of median values. This trend indicates that the network becomes more consistent in terms of its DRES capacity acceptance as the number of DRES installations rises.

The distribution analysis of the maximum DRES penetration level at the CIGRE MV network with different voltage control methods is illustrated in Fig. 10 and Table 1. This analysis aims to evaluate the impact of voltage control methods on the maximum acceptable penetration level. Simulation results indicate that when using the constant Q control method, to ensure voltage violations remain within the acceptable limits, a conservative choice for DRES power penetration level would be 9 MW. However, as seen in Fig. 10, only a small fraction of all scenarios (0.75%) have a penetration level below 10 MW with the constant Q control method. Therefore, while selecting the minimum value from all scenarios as the limit for DRES penetration level may be the safest option, it is not the most sustainable choice.

In distinct scenarios characterized by specific capacity allocations and installation locations, the grid can accommodate up to 48 MW of DRES utilizing the Constant Q control method, which extends to 65 MW under the Constant $Q(V)$ control method shown in Table 1. Given that the DRES installed capacity allocation and installation locations are randomly selected, the decision by the DSO regarding the DRES installation and penetration level hinges on striking a balance between the extent of DRES penetration and the associated risk of voltage violations. For instance, if we opt for the $qut1$ value, although it may result in a voltage violation probability of 75%, it permits an increase in DRES capacity up to 14 MW. This effectively underscores the flexible and strategic trade-off between maximizing renewable energy integration and ensuring network reliability and stability.

To investigate the impact of the number of installed DRES on their acceptable capacity, we conducted a distribution analysis of 1600 scenarios with different numbers of installed DRES. The histogram for various DRES installation numbers is displayed in Fig. 11, while the analysis data is presented in Table 2. The table and figure show that as the number of installed DRES increases, the distribution of maximum installed capacity becomes tighter. With more DRES integrated into the network, the total DRES power increases; however, the rate of increment appears to diminish. Due to the limited number of nodes in

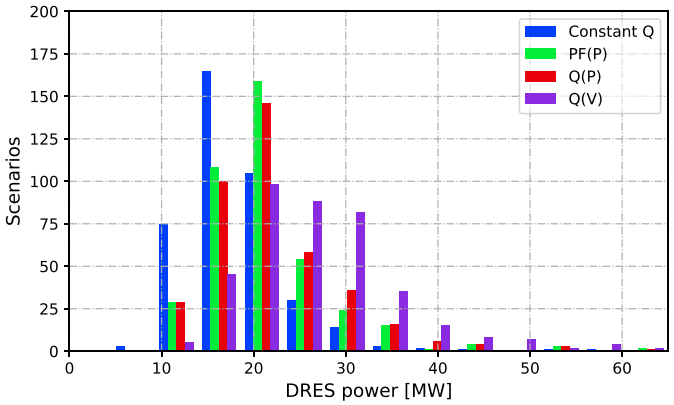

Fig. 10. The histogram of the maximum DRES penetration level for different voltage control methods.

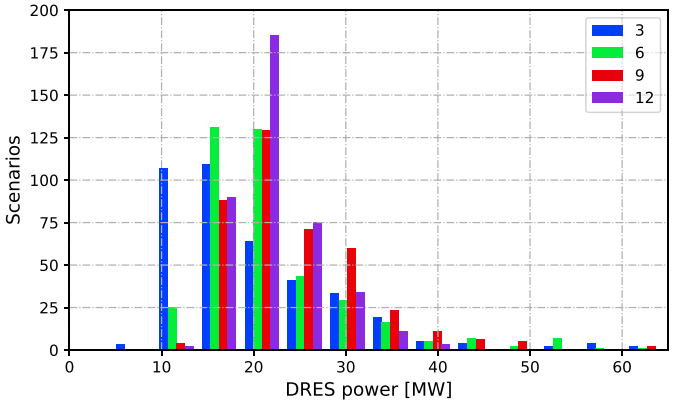

Fig. 11. The histogram of the maximum DRES penetration level for different DRES installed numbers.

the CIGRE MV grid, we cannot increase the number of DRES beyond 14 to verify if this trend persists. To further explore this trend, the IEEE LV feeder grid, which has a greater number of nodes, can be utilized for analysis.

3.1.2. Case study with IEEE European Test Feeder grid

This section analyzes 4000 scenarios with different DRES installation numbers and control methods in the IEEE European Test Feeder grid. The distribution of maximum accepted DRES capacity in the IEEE European Test Feeder grid, considering different control methods, is depicted in Fig. 12. Compared to the $PF(Q)$, $Q(P)$, and $Q(V)$ control methods, the constant Q control method appears to be less effective.

The distribution of maximum accepted DRES capacity in the IEEE European Test Feeder grid with varying installed DRES numbers is illustrated in Fig. 13. This exhibits a similar pattern to the simulation results in the CIGRE MV network. As more DRES are integrated into the network, the overall DRES power increases, but the rate of increment diminishes.

3.1.3. Reliability analysis with one-year simulation

Following the conclusions drawn above, the acceptable DRES installed capacity in the network can be determined using a given control method and the DRES number. Although a large number of simulated scenarios are analyzed, voltage violations still occur due to dynamic changes in the load profile and DRES-generated power. To assess the risk of voltage violations in the MV CIGRE network, we perform a

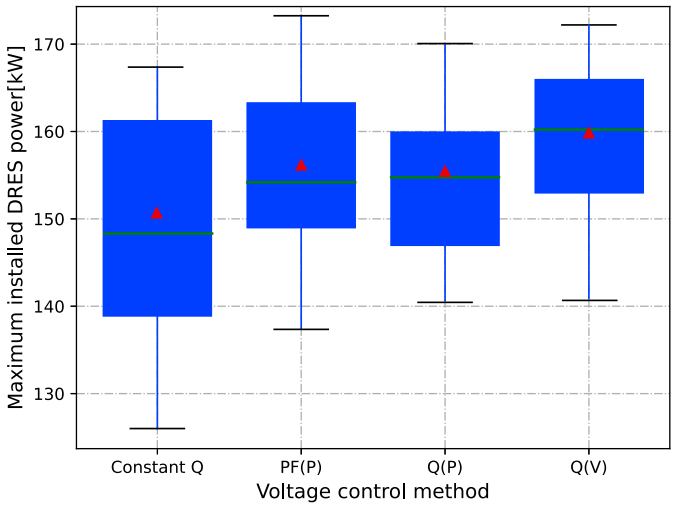

Fig. 12. The maximum DRES penetration level in IEEE European Test Feeder grid with different DRES control methods.

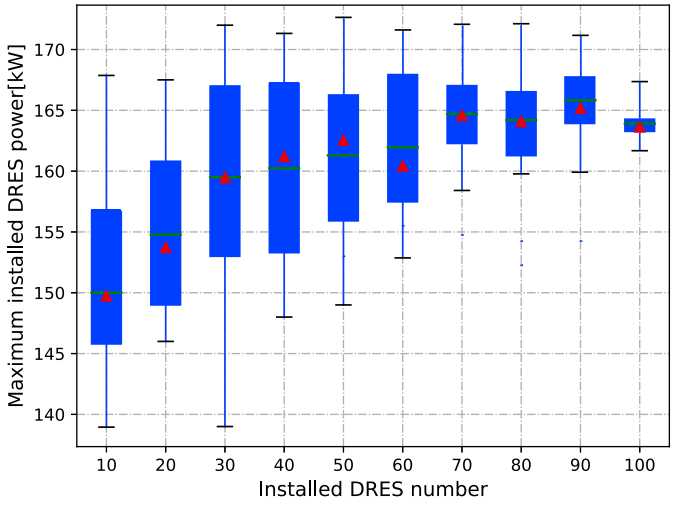

Fig. 13. The maximum DRES penetration level in IEEE European Test Feeder grid with different DRES penetration numbers.

Table 1
Influence of control methods on DRES penetration in MW.

Control method	*min*	*qut*1	*μ*	*qut*3	*max*
Constant Q	9	14	18	21	48
$PF(P)$	10	17	22	24	61
$Q(P)$	10	17	22	25	62
$Q(V)$	12	21	28	31	65

Table 2
Influence of DRES number on DRES penetration in MW.

DRES number	*min*	*qut*1	*μ*	*qut*3	*max*
3	9	13	21	25	61
6	11	17	22	25	62
9	12	19	24	28	65
12	13	19	22	25	39

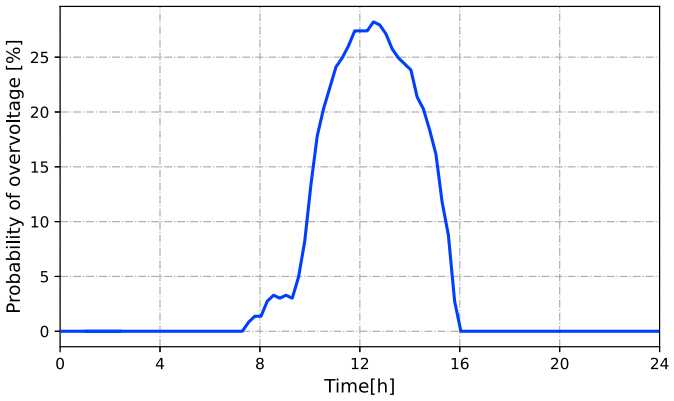

Fig. 14. The over-voltage probability of Node 11 in August.

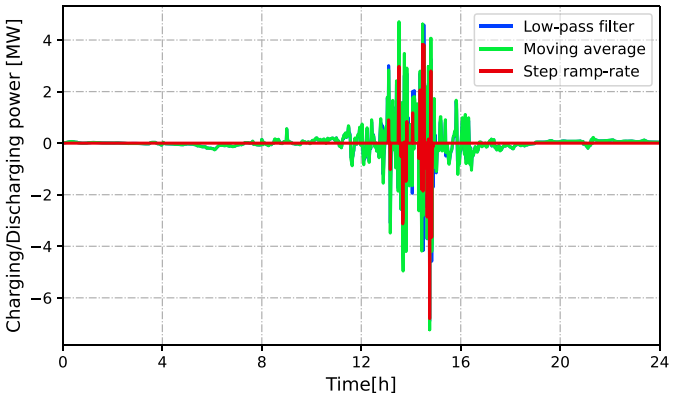

Fig. 15. Charging/Discharging power of the *battery1* (positive value for charging; negative value for discharging).

one-year simulation with a 15-minute time-step. The DRES installed capacity in the Cigre MV network is set to 28 MW (mean value of $Q(V)$ control method with 9 DRES in Fig. 9) located at buses 1, 4, 5, 7, 8, 10, 11, 12, and 14. In the one-year simulation, the risk of voltage violations is only 5.68%, which occurs only at node 11 (with a voltage rise problem). Following EN 50160 standard [22], Under normal operating conditions, 95% of the time over a period of one week should keep within the voltage limit. Thus, a voltage violation rate of 5.68% over a one-year simulation is within acceptable bounds according to the EN 50160 standard. The risk of over-voltage is at its peak in August, specifically at 12:30 PM. There are 9 days in August that have the over-voltage problem (with the probability 28.22%) at 12:30 PM. The over-voltage probability of Node 11 in August is shown in Fig. 14, and the most severe instance of this issue observed was a voltage surge to 1.0504 pu.

The simulation results show that our stochastic simulation-based method can successfully determine the maximum DRES penetration level based on the different DRES numbers and control methods. We perform the statistical analysis for many simulated scenarios using a voltage control method to guarantee the DRES penetration within the maximum allowed limits. We can determine the DRES penetration level based on our probability distribution analysis. Moreover, the proposed stochastic simulation-based method can explore the voltage violation risk for a given network with the desired installed DRES power, DRES locations, and specified voltage control method. By performing a simulation over a long period (in this paper, we perform the one-year simulation), we can obtain the risk of voltage violations and the time in which the risk of violations is concentrated for each node.

Table 3
Calculated MV CIGRE network BESS sizing.

Control method	BESS capacity [MWh]	P_{ch}^{max} [MW]	P_{dch}^{max} [MW]
Low-pass filter	2.00	4.57	6.89
Moving average	2.10	4.70	7.24
Step ramp-rate	0.60	3.82	6.79

3.2. Case study for BESS capacity determination

In this section, we conduct a case study to determine the required BESS capacity for power smoothing. We utilize the same scenario described in Section 3.1.1, which involves the installation of 28 MW DRES using the $Q(V)$ control method, to carry out the power smoothing case study. The Moving Average method, Low-pass Filter [17], and a specific Step Ramp-rate Control Strategy [18] are employed to achieve power smoothing. We define the ramp-rate limit as $\Delta P/min \leq 10\%$ of the total DRES rated power [23,24], which amounts to 2.8 MW per minute.

The simulation results show the required power smoothing BESS capacity for each method in Table 3, where P_{ch}^{max} represents the maximum charging power requirement, and P_{dch}^{max} denotes the maximum discharging power requirement. To achieve the ramp-rate limit of 10% per minute, a window size of 4 min is calculated as the moving window for the Moving Average method, while a normalized cutoff frequency of 0.21 is employed for the Low-pass Filter method. From the results, these three power smoothing methods do not show significant differences in the maximum requirements of charge and discharge rated power. However, the Step Ramp-rate Control Strategy requires much less BESS capacity compared to the Low-pass Filter and Moving Average methods. During simulations, the C-rate limitation was not explicitly included. Therefore, when setting the BESS, the required BESS capacity, P_{ch}^{max} and P_{dch}^{max}, all need to be taken into consideration.

Since the PV-generated power and load consumption exhibit a similar pattern each day, we perform simulations iteratively to determine the BESS capacity requirements for each day. For one day with the profile shown in Fig. 8. The BESS charging/discharging power is displayed in Fig. 15 during the simulation to limit the ramp-rate within limitation after power smoothing.

The BESS is primarily active during daytime hours when the DRES generates significant power because most power fluctuations occur during that period. The corresponding BESS SoC from 8:00 AM to 8:00 PM on that day is depicted in Fig. 16. We can observe that the SoC of the BESS maintains an acceptable value throughout the day, demonstrating the effectiveness of our model. The power before and after power smoothing for different methods is shown in Fig. 17. The black line represents the power through line *Line Feeder 1*, which is the power without power smoothing. The blue line indicates the power through transformer *T Feeder 1* when the Low-pass Filter method is applied to smooth the power in *Feeder 1*.

To accurately determine BESS capacity, it is critical to conduct a simulation spanning a minimum of one year, considering the variation in seasons and weather conditions. The research presented in this paper encompasses such a one-year simulation. As depicted in Fig. 18, the daily BESS capacity requirements vary throughout the year. Specifically, the requirements in January, February, November, and December are lower due to decreased DRES-generated power. Furthermore, the BESS capacity requirements spike noticeably on days with significant intermittency in DRES-generated power.

A comparative analysis of the Low-pass Filter, Moving Average, and Step Ramp-rate methods reveals that the latter necessitates substantially less BESS capacity. In order to meet the power smoothing goal all year round, the Low-pass Filter, Moving Average, and Step Ramp-rate methods necessitate BESS capacities of 4.18 MWh, 3.70 MWh, and 1.01 MWh, respectively. However, tolerating brief periods of non-adherence to the power smoothing target can significantly reduce the requisite

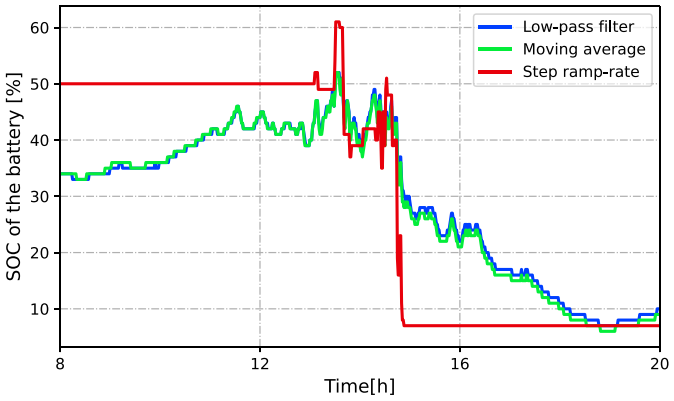

Fig. 16. Soc of *battery1* during one day.

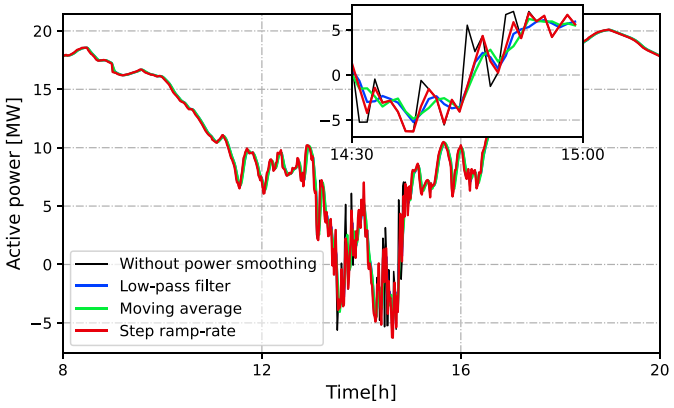

Fig. 17. Power smoothing performance during one day at *Feeder 1*.

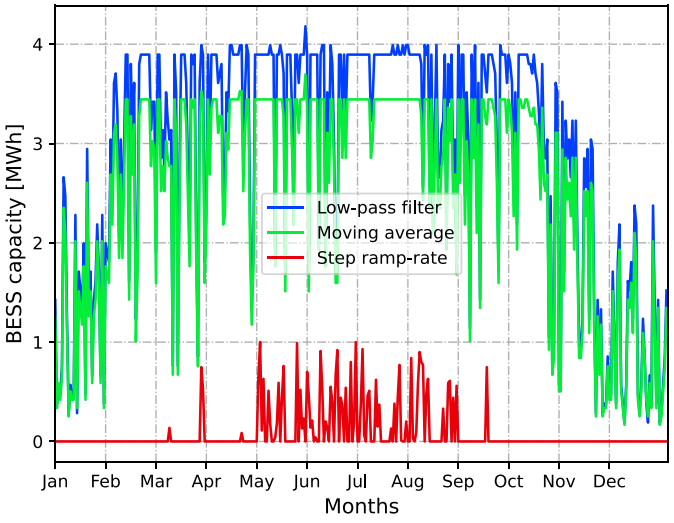

Fig. 18. BESS capacity requirements at each day during one year.

BESS capacity. For instance, if a 10% deviation from the power smoothing target is permissible, the necessary BESS capacities diminish to 3.89 MWh, 3.44 MWh, and 0.45 MWh, respectively. The C-rate, defined as the rate at which the battery is charged or discharged relative to its maximum capacity, is crucial for ensuring that the BESS can meet dynamic power requirements without degradation. Therefore, when sizing the BESS, it is essential to ensure that the C-rate remains within the manufacturers' recommended limits to guarantee the longevity and efficiency of the BESS.

Table 4
BESS capacity sensitivity analysis considering the deviation allowable.

Deviation possibility	Lower-pass filter	Moving average	Step ramp-rate
10%	3.89	3.44	0.45
5%	3.95	3.45	0.63
2%	3.99	3.47	0.82
1%	4.01	3.50	0.92
0%	4.18	3.69	1.01

The sensitivity analysis, as shown in Table 4, elucidates the impact of varying allowable deviations from the power smoothing target on the BESS capacity requirements for the three power smoothing methods. Notably, the Step Ramp-rate method consistently requires the least BESS capacity, attesting to its efficiency in power smoothing. As the acceptable deviation shrinks, signifying stricter power quality standards, all methods demand increased BESS capacity, thereby underscoring the trade-off between power quality and BESS capacity requirements. Moreover, the Step Ramp-rate method exhibits more significant reductions in BESS capacity requirements than the Low-pass Filter and Moving Average methods.

The simulation results demonstrate that our stochastic simulation-based approach effectively compares the performance of various power smoothing methods and performs BESS sizing using probability density analysis of at least one year of simulation results. By considering different power smoothing methods, the optimal BESS capacity can be determined by striking a balance between economic considerations and power smoothing performance. This approach ensures a more informed decision-making process for selecting and implementing suitable power smoothing techniques and BESS capacity in renewable energy systems.

4. Conclusion

This paper examined the effects of increased DRES penetration on voltage violations and evaluated the necessary BESS capacity for power smoothing in distribution networks. Our analysis demonstrated that the Constant $Q(V)$ control method yielded superior results compared to other control methods, and an increased number of DRES installations resulted in a tighter distribution of DRES maximum installed capacity. A one-year simulation indicated that the risk of voltage violations could be minimized to 5.68% with an appropriately designed DRES installation and control strategy. The case study for determining BESS capacity for power smoothing revealed that the Step Ramp-rate Control Strategy necessitated significantly lower BESS capacity compared to other methods while preserving power quality. These findings can assist network operators and planners in efficiently integrating renewable energy sources and storage systems for a reliable and sustainable power grid.

CRediT authorship contribution statement

Aihui Fu: Writing – original draft, Methodology, Conceptualization. **Aleksandra Lekić:** Writing – review & editing, Writing – original draft, Conceptualization. **Kyriaki-Nefeli D. Malamaki:** Writing – review & editing, Conceptualization. **Georgios C. Kryonidis:** Writing – review & editing, Formal analysis, Conceptualization. **Juan M. Mauricio:** Writing – review & editing, Conceptualization. **Charis S. Demoulias:** Writing – review & editing, Conceptualization. **Peter Palensky:** Supervision. **Miloš Cvetković:** Writing – review & editing, Supervision, Funding acquisition, Conceptualization.

Declaration of competing interest

The authors declare that they have no known competing financial interests or personal relationships that could have appeared to influence the work reported in this paper.

Data availability

Data will be made available on request.

Acknowledgments

This work was supported by the European Union, Horizon 2020 project EASYRES, grant agreement: 764090.

References

[1] Mlilo N, Brown J, Ahfock T. Impact of intermittent renewable energy generation penetration on the power system networks–A review. Technol Econ Smart Grids Sustain Energy 2021;6(1):1–19. http://dx.doi.org/10.1007/s40866-021-00123-w.

[2] IEEE standard for interconnection and interoperability of distributed energy resources with associated electric power systems interfaces. In: IEEE Std 1547-2018 (Revision of IEEE Std 1547-2003). 2018, p. 1–138.

[3] Bedawy A, Yorino N, Mahmoud K, Zoka Y, Sasaki Y. Optimal voltage control strategy for voltage regulators in active unbalanced distribution systems using multi-agents. IEEE Trans Power Syst 2020;35(2):1023–35. http://dx.doi.org/10.1109/TPWRS.2019.2942583.

[4] Fu A, Cvetković M, Palensky P. Distributed cooperation for voltage regulation in future distribution networks. IEEE Trans Smart Grid 2022;13(6):4483–93. http://dx.doi.org/10.1109/TSG.2022.3191389.

[5] Sharma S, Niazi KR, Verma K, Thokar RA. Bilevel optimization framework for impact analysis of DR on optimal accommodation of PV and BESS in distribution system. Int Trans Electr Energy Syst 2019;29(9):e12062. http://dx.doi.org/10.1002/2050-7038.12062.

[6] Demoulias CS, Malamaki K-ND, Gkavanoudis S, Mauricio JM, Kryonidis GC, Oureilidis KO, Kontis EO, Martinez Ramos JL. Ancillary services offered by distributed renewable energy sources at the distribution grid level: An attempt at proper definition and quantification. Appl Sci 2020;10(20). http://dx.doi.org/10.3390/app10207106.

[7] de Siqueira LMS, Peng W. Control strategy to smooth wind power output using battery energy storage system: A review. J Energy Storage 2021;35:102252. http://dx.doi.org/10.1016/j.est.2021.102252.

[8] Malamaki K-ND, Casado-Machado F, Barragán-Villarejo M, Gross AM, Kryonidis GC, Martinez-Ramos JL, Demoulias CS. Ramp-rate control of DRES employing supercapacitors in distribution systems. In: 2021 international conference on smart energy systems and technologies. SEST, 2021, p. 1–6. http://dx.doi.org/10.1109/SEST50973.2021.9543116.

[9] Alam MJE, Muttaqi KM, Sutanto D. A novel approach for ramp-rate control of solar PV using energy storage to mitigate output fluctuations caused by cloud passing. IEEE Trans Energy Convers 2014;29(2):507–18. http://dx.doi.org/10.1109/TEC.2014.2304951.

[10] Syed MA, Khalid M. Neural network predictive control for smoothing of solar power fluctuations with battery energy storage. J Energy Storage 2021;42:103014. http://dx.doi.org/10.1016/j.est.2021.103014.

[11] Martins J, Spataru S, Sera D, Stroe D-I, Lashab A. Comparative study of ramp-rate control algorithms for PV with energy storage systems. Energies 2019;12(7). http://dx.doi.org/10.3390/en12071342.

[12] Tahir H, Park D-H, Park S-S, Kim R-Y. Optimal ESS size calculation for ramp rate control of grid-connected microgrid based on the selection of accurate representative days. Int J Electr Power Energy Syst 2022;139:108000. http://dx.doi.org/10.1016/j.ijepes.2022.108000.

[13] DIgSILENT. PowerFactory 2024 documentation. 2024, URL https://www.digsilent.de.

[14] European Committee for Electrotechnical Standardization (CENELEC). Requirements for generating plants to be connected in parallel with distribution networks - Part 1: Connection to a LV distribution network - Generating plants up to and including Type B. 2019, EN 50549-1:2019 Standard.

[15] European Committee for Electrotechnical Standardization (CENELEC). Requirements for generating plants to be connected in parallel with distribution networks - Part 2: Connection to a MV distribution network - Generating plants up to and including Type B. 2019, EN 50549-2:2019 Standard.

[16] Gkavanoudis SI, Malamaki K-ND, Kontis EO, Demoulias CS, Shekhar A, Mushtaq U, Venu SB. Provision of ramp-rate limitation as ancillary service from distribution to transmission system: Definitions and methodologies for control and sizing of central battery energy storage system. J Mod Power Syst Clean Energy 2023;11(5):1507–18. http://dx.doi.org/10.35833/MPCE.2022.000595.

[17] Liu H, Peng J, Zang Q, Yang K. Control strategy of energy storage for smoothing photovoltaic power fluctuations. IFAC-PapersOnLine 2015;48(28):162–5. http://dx.doi.org/10.1016/j.ifacol.2015.12.118.

[18] Malamaki K-ND, Marano A, Mushtaq U, Cvetkovicć M. D1.3 1st report on the reactive power control algorithm for converter-interfaced DRES/BESS and analytical tool for parametric BESS sizing for low-frequency power smoothing. Jul. 2019, H2020 EASY-RES Project Deliverable.

[19] Barsali S, et al. Benchmark Systems for Network Integration of Renewable and Distributed Energy Resources. 2014.

[20] Khan MA, Hayes BP. A reduced electrically-equivalent model of the IEEE European low voltage test feeder. In: 2022 IEEE power & energy society general meeting. PESGM, 2022, p. 1–5. http://dx.doi.org/10.1109/PESGM48719.2022.9916806.

[21] Liander. Liander open data. 2022, URL https://www.liander.nl/partners/datadiensten/open-data.

[22] Standard B, et al. Voltage characteristics of electricity supplied by public distribution networks. 2007, BS EN.

[23] National Renewable Energy Laboratory. Puerto rico electric power authority's minimum technical renewables interconnection requirements. 2012.

[24] Ai X, Li J, Fang J, Yao W, Xie H, Cai R, Wen J. Multi-time-scale coordinated ramp-rate control for photovoltaic plants and battery energy storage. IET Renew Power Gener 2018;12(12):1390–7. http://dx.doi.org/10.1049/iet-rpg.2018.5190.